Channel-Dependent Scheduling of an Uplink SC-FDMA System with Imperfect Channel Information

Hyung G. Myung*, Kyungjin Oh†, Junsung Lim‡, and David J. Goodman†

* Qualcomm/Flarion
Bedminster, NJ, USA

† Polytechnic University
Brooklyn, NY, USA

‡ Samsung Electronics
Suwon, South Korea

***Abstract*— Channel-dependent scheduling (CDS) can increase the data throughput of a cellular system by exploiting multi-user diversity and frequency selectivity in the channel. In this paper, we investigate the impact of imperfect channel state information (CSI) on CDS. Specifically, we analyze the data throughput of an uplink single carrier FDMA (SC-FDMA) system with uncoded adaptive modulation and CDS when there is a CSI feedback delay. We consider distributed and localized subcarrier mapping schemes for resource allocation. We show that localized subcarrier mapping yields highest aggregate data throughput when we use CDS. However, we also show that localized mapping is very sensitive to the quality of CSI and the capacity gain quickly decreases when the channel changes rapidly. For high mobility users, distributed mapping with static round-robin scheduling is more suitable.**

***Index Terms*—resource scheduling, single carrier FDMA, adaptive modulation, feedback delay**

I. INTRODUCTION

In broadband multi-user communications, the channel gain of each user is time-dependent and frequency-dependent. At any time, frequency bands in deep fading for one user may have low attenuation for other users. A resource scheduler in the base station can assign the time-frequency resources to a favorable user which will increase the total system throughput [1], [2], [3]. We refer to this adaptive resource scheduling method as channel-dependent scheduling (CDS).

Another way to exploit the variability in the channel is adaptive modulation and coding (AMC) . AMC dynamically adapts the modulation constellation and the channel coding rate depending on the channel condition and thus improves the energy efficiency and the data rate [4], [5]. By applying AMC to subbands or subcarriers, we can improve the link quality and increase the data rate for time and frequency selective fading channels.

In this paper, we investigate CDS for an uplink single carrier FDMA (SC-FDMA) system with imperfect channel information. We first give a general overview of the SC-FDMA system we have studied. Then, we explain the two subcarrier mapping schemes, *distributed* and *localized*, available for resource scheduling. In the next section, we investigate the impact of imperfect channel state information (CSI) on CDS. Specifically, we use simulations to study the data throughput of an SC-FDMA system with uncoded adaptive modulation and CDS when there is a feedback delay.

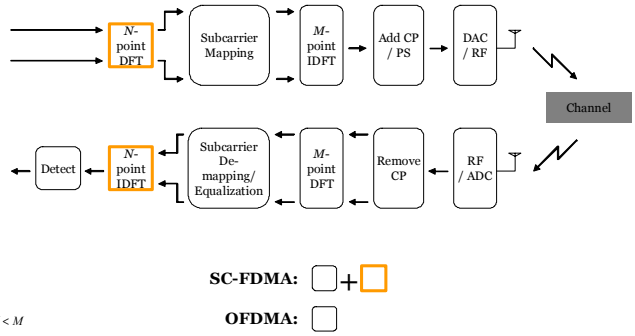

Figure 1: Transmitter and receiver structure of an SC-FDMA system.

II. SINGLE CARRIER FDMA (SC-FDMA)

SC-FDMA, which utilizes single carrier modulation and frequency domain equalization, is a technique that has similar throughput and essentially the same overall structure as OFDMA [6]. One advantage over OFDMA is that the SC-FDMA signal has lower peak-to-average power ratio (PAPR) because of its inherent single carrier structure [7]. SC-FDMA has attracted attention as an alternative to OFDMA, especially in uplink communications where lower PAPR benefits the mobile terminal in terms of transmit power efficiency. SC-FDMA has been adopted as the uplink multiple access scheme for the 3rd Generation Partnership Project Long Term Evolution (3GPP LTE) [8].

Figure 1 illustrates the transmitter and receiver structure of SC-FDMA. The transmitter of an SC-FDMA system first groups the modulation symbols into blocks each containing N symbols. Next it performs an N-point discrete Fourier transform (DFT) to produce a frequency domain representation of the input symbols. It then maps each of the N-DFT outputs to one of the M ($> N$) orthogonal subcarriers that can be transmitted. The collection of N subcarriers assigned to the DFT output is referred to as a *chunk*. An M-point inverse DFT

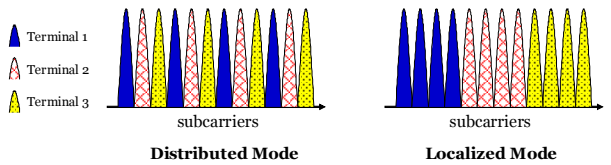

Figure 2: Subcarrier mapping schemes; distributed and localized.

(IDFT) transforms the subcarrier amplitudes to a complex time domain signal.

The transmitter performs two other signal processing operations prior to transmission. It inserts a set of symbols referred to as a cyclic prefix (CP) in order to provide a guard time to prevent inter-block interference due to multi-path propagation. The transmitter also performs a linear filtering operation referred to as pulse shaping in order to reduce out-of-band signal energy. The receiver transforms the received signal into the frequency domain via DFT, de-maps the subcarriers, and then performs frequency domain equalization. Most of the well- known time domain equalization techniques, such as minimum mean square error (MMSE) equalization, decision feedback equalization (DFE), and turbo equalization, can be applied to the frequency domain equalization [9], [10], [11], [12]. The equalized symbols are transformed back to the time domain by means of an IDFT, and detection and decoding take place in the time domain.

III. Subcarrier Mapping Methods

Figure 2 shows two methods of assigning subcarriers to DFT outputs: distributed subcarrier mapping (DFDMA) and localized subcarrier mapping (LFDMA). In the case of LFDMA, the DFT outputs are assigned to adjacent subcarriers. With DFDMA, DFT outputs are distributed over the entire bandwidth with zero amplitude assigned to the unused subcarriers. When M/N is an integer, the occupied subcarriers are equally spaced and the DFDMA assignment is referred to as Interleaved FDMA (IFDMA). With IFDMA, the transmitter can modulate the signal strictly in the time domain without the use of DFT and IDFT [13].

From a resource allocation point of view, subcarrier mapping methods are further divided into static and channel-dependent scheduling (CDS) methods. CDS assigns subcarriers to users according to the channel frequency response of each user. For both scheduling methods, distributed subcarrier mapping provides frequency diversity because the transmitted signal is spread over the entire bandwidth. With DFDMA, CDS incrementally improves performance. By contrast, CDS is of great benefit with LFDMA because it can exploit the frequency selectivity of the channel to assign terminals to frequency bands with favorable propagation conditions.

IV. Channel-Dependent Scheduling of an Uplink SC-FDMA System with Outdated CSI

In [14] and [15], we investigated channel-dependent resource scheduling for an SC-FDMA system in uplink communications assuming perfect knowledge of channel state information

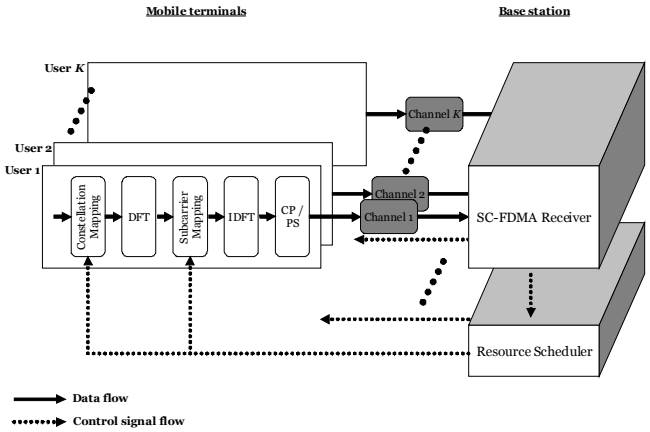

Figure 3: Block diagram of an uplink SC-FDMA system with adaptive modulation and CDS for K users.

(CSI). Specifically, we analyzed the capacity gains from CDS for the two different flavors of subcarrier mapping of SC-FDMA using utility-based scheduling [16]. Our numerical simulation results showed that CDS increases system throughput by up to 80% relative to static scheduling for localized subcarrier mapping scheme but the increase is only 26% for distributed mapping scheme.

In a practical wireless system, CSI is often not known at all or only part of the information is available due to limited feedback and channel estimation errors. Also, the CSI may become outdated because of the feedback delay. In a centralized resource management scheme, the base station performs uplink resource assignment based on the channel quality and transmits the transmission parameter information to the mobile terminals. A delay in the feedback mechanism is inevitable in a practical system and the feedback delay has a major impact on the system performance especially when the channel is fading rapidly.

In this section, we investigate the impact of imperfect CSI on CDS in uplink communications by considering outdated CSI due to feedback delay. We assume the channel estimation is perfect and also assume there is no error during the feedback signaling. Since there is no general closed form for the capacity with outdated CSI, we simulate an SC-FDMA system with uncoded adaptive modulation to measure the data throughput.

A. Uplink SC-FDMA System with Adaptive Modulation and CDS

Figure 3 describes the multi-user uplink transmission system under investigation. There are K terminals with mutually independent channel transfer functions. To provide the base station with channel state information, the terminals transmit pilot signals on subcarriers spanning the entire frequency band. Upon acquiring the channel information for all terminals the scheduler at the base station first searches for a set of users that maximizes the total capacity. Next, for each user, it decides the modulation constellation based on the SNR of the subcarrier chunk allocated to the user. The scheduler then alloates a chunk of N subcarriers to each terminal and transmits the chunk allocation and modulation information to each user.

When there is a delay in the feedback channel, the chunk

allocations to users and the modulation constellations of each user may no longer be optimal by the time the terminals transmit their signals. These two factors decrease the total capacity when the channels vary rapidly with time.

In our analysis, we introduce a time delay between the time of the channel estimation ($t = t_1$) and the actual time of data transmission from the mobile terminals ($t = t_2$). The time difference is $\Delta t = t_2 - t_1$ We consider a quasi-static multi-path fading channel in which channel response is constant over a transmission time interval (TTI) but changes from one TTI to the next. For a Rayleigh fading channel, we represent the change in channel conditions between two TTIs by the correlation coefficient:

$$\rho(\Delta t) = J_0(2\pi v \Delta t / \lambda) = J_0(2\pi f_D \Delta t) \quad (1)$$

where $J_0(\bullet)$ is the zero-order Bessel function, $f_D = v/\lambda$ is the maximum Doppler frequency, v is the velocity of the mobile terminal, and λ is the wavelength of the carrier signal [17].

We model the multi-path fading channel at t_1 with an R-path discrete time channel impulse response, $h^{(t_1)}(n)$, as follows.

$$h^{(t_1)}(n) = \sum_{r=0}^{R-1} A \cdot \sqrt{P_{rel}(\tau_r)} \cdot w_r^{(t_1)} \cdot \delta\left(n - \frac{\tau_r}{T_s}\right) \quad (2)$$

where $\{w_r^{(t_1)}\}$ is a set of zero mean complex Gaussian i.i.d. noise process, τ_r is the propagation delay of path r, T_s is the symbol duration, A is a normalization parameter such that the average power of the channel is 1, $P_{rel}(\tau_r)$ is the relative power of the delay profile model for path r, and $\delta(n)$ is the discrete time Dirac-delta function. Note that $\{\tau_r\}$'s are integer-multiples of T_s.

Using (1), we can generate the multi-path fading channel at t_2, $h^{(t_2)}(n)$, as follows.

$$h^{(t_2)}(n) = \sum_{r=0}^{R-1} A \cdot \sqrt{P_{rel}(\tau_r)} \cdot w_r^{(t_2)} \cdot \delta(n - \frac{\tau_r}{T_s}) \quad (3)$$

and

$$w_r^{(t_2)} = \rho(\Delta t) \cdot w_r^{(t_1)} + \sqrt{1 - \rho^2(\Delta t)} \cdot n_r \quad (4)$$

where n_r is a zero mean complex Gaussian noise process.

We will use (2) and (3) to analyze the effect of the outdated channels on our system.

In [14], we derived the SNR of user k, γ_k, as follows based on [18] for an MMSE equalizer when a set of subcarriers $I_{sub,k}$ is assigned to the user.

$$\gamma_k = \left(\frac{1}{\frac{1}{N} \sum_{i \in I_{sub,k}} \frac{\gamma_{i,k}}{\gamma_{i,k} + 1}} - 1 \right)^{-1} \quad (5)$$

where N is the number of subcarriers allocated to the user and $\gamma_{i,k}$ is the SNR of subcarrier i for user k. For equal power allocation scheme, we can express $\gamma_{i,k}$ as

$$\gamma_{i,k} = \frac{(P_k / N) \cdot H_{i,k}}{\sigma_i^2} \quad (6)$$

where P_k is the total transmit power of user k, $H_{i,k}$ is the channel gain of subcarrier i for user k, and σ_i^2 is the noise power of subcarrier i. H is the frequency domain representation of $h(n)$.

In our simulations, we investigate the effect of the time delay during feedback in the following manner. We first calculate the received SNRs for the subcarrier allocations and select the modulation constellations based on the channels at time t_1 and then calculate the received SNRs for the throughput calculations based on the channels at time t_2. The details of the near-optimum subcarrier allocation method are in [14].

For the numerical simulations, we consider the following setup and assumptions which are typical of a 3GPP LTE system:

- Carrier frequency: 2 GHz.
- Transmission bandwidth: 5 MHz.
- Duration of a transmission time interval (TTI): 0.5 ms.
- Blocks per TTI: 7. We assume there is no CP in a block.
- The size of the subcarrier chunk is the same among all users and each user occupies only one subcarrier chunk.
- The number of users is K, the total number of subcarriers M, the size of a chunk N, the number of chunks Q, and $M = Q \cdot N$.
- Channel model: 3GPP TU6 i.i.d. quasi-static Rayleigh fading channel [19]. We assume that the channel is constant during the duration of a TTI. We also assume that all the users have the same average path loss to the base station.
- Modulation format: Quadrature amplitude modulation (QAM). We consider S-QAM where $S = 2^B$ and B is the number of bits per symbol. We have 8 classes of QAM where $B \in \{1, 2, \ldots, 8\}$. $B = 1$ corresponds to BPSK and $B = 2$ to QPSK.
- We assume equal transmit power and equal receive noise power for all users.

B. System Throughput Calculation

We define the system throughput as the number of information bits per second received without error. Let user k be assigned S_k-QAM where $S_k = 2^{B_k}$ and B_k is the number of bits per symbol. Then we express the system throughput TP_k for user k as follows [20].

$$TP_k = \frac{7 \cdot N \cdot B_k}{T_{TTI}} \cdot PSR(S_k, \gamma_k) \quad (7)$$

where T_{TTI} is the duration of a TTI, γ_k is the received SNR for user k, and $PSR(\bullet)$ is the packet success rate (PSR) which we define as the probability of receiving an information packet correctly. The aggregate throughput TP_{total} is the sum of the K individual throughput measures in (7).

For an uncoded packet with a size of L bits, PSR becomes

$$PSR(S, \gamma) = \{1 - P_e(S, \gamma)\}^L \quad (8)$$

where $P_e(S, \gamma)$ is the BER for a given constellation size S and SNR γ.

For an additive white Gaussian noise (AWGN) channel with S-QAM modulation and ideal coherent detection, we can upper-bound $P_e(S, \gamma)$ as follows [21].

$$P_e(S, \gamma) \le 0.2 e^{\frac{-1.5\gamma}{(S-1)}} \quad (9)$$

Using this upper bound, PSR in (8) becomes

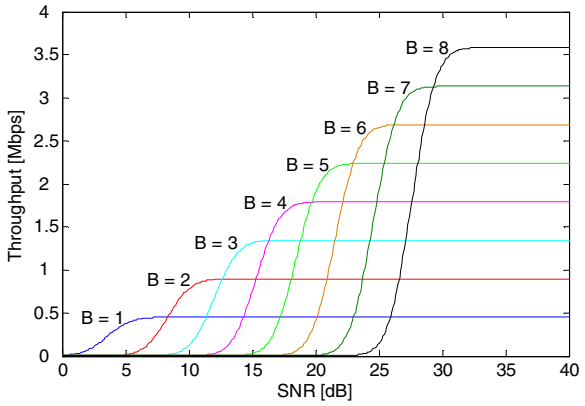

Figure 4: System throughput vs. SNR for the 8 classes of QAM. *B* is the number of bits per symbol.

TABLE 1: SNR BOUNDARIES FOR ADAPTIVE MODULATION.

SNR (dB)	Bits per symbol (*B*)	Modulation
> 8.7	1	BPSK
8.7 ~ 13.0	2	QPSK
13.0 ~ 16.7	3	8-QAM
16.7 ~ 20.0	4	16-QAM
20.0 ~ 23.3	5	32-QAM
23.3 ~ 26.6	6	64-QAM
26.6 ~ 29.6	7	128-QAM
29.6 <	8	256-QAM

$$PSR(S,\gamma)=\left\{1-0.2e^{\frac{-1.5\gamma}{(S-1)}}\right\}^{L} \tag{10}$$

and the system throughput for user k becomes

$$TP_k=\frac{7\cdot N\cdot B_k}{T_{TTI}}\cdot\left\{1-0.2e^{\frac{-1.5\gamma_k}{(S_k-1)}}\right\}^{L} \tag{11}$$

Then, the total system throughput for K users is

$$TP_{total}=\sum_{k=1}^{K}TP_k \tag{12}$$

Figure 4 shows the system throughput vs. SNR for the 8 classes of QAM. We use L = 100 bits per packet and N = 32 subcarriers per chunk. Based on Figure 4, we set the SNR boundaries for the adaptive modulation. Table 1 describes the SNR boundaries for our analysis.

C. *Numerical Results*

Figures 5, 6, and 7 show the results of the Monte Carlo simulations. The total number of subcarriers is M = 256. There are Q = 16 frequency chunks and the number of subcarriers per chunk is N = 16. There are K = 64 users with 16 users transmitting simultaneously in each TTI. We perform 2000 independent iterations of the simulation. One iteration refers to a transmission over one TTI and its corresponding throughput calculation.

Figure 5 shows the aggregate throughputs with CDS and adaptive modulation for mobile speeds of 3 km/h and 60 km/h. For 3 km/h, the feedback delay does not affect the system throughput. However, at 60 km/h, the throughput degrades as the feedback delay increases and the degradation is most significant for LFDMA with CDS. Another interesting observation is that the static round-robin scheduling also suffers from throughput decrease. This is due to the fact that even though there is no chunk allocation mismatch, outdated CSI causes the adaptive modulation to be mismatched with the current channel condition.

Figure 6 shows the aggregate throughput with CDS for mobile speed of 60 km/h and constant modulation (16-QAM) instead of adaptive modulation. It further verifies the observation in Figure 5 (b) for static scheduling that the cause of the throughput decrease is the adaptive modulation process. We do not see any throughput decrease for the static scheduling when we use constant modulation.

Figure 7 shows the aggregate throughput with CDS and adaptive modulation with feedback delay of 3 ms and different mobile speeds. We can see the performance impact of the mobility of the user on each type of scheduling method. Similarly with Figure 5 (b), LFDMA with CDS suffers the most throughput decrease when the mobile speed is high.

V. CONCLUSIONS

In this paper, we investigate channel-dependent scheduling (CDS) for an uplink single carrier FDMA (SC-FDMA) system. Specifically, we analyze the capacity gains from CDS for the two different flavors of subcarrier mapping of SC-FDMA and we look into the impact of imperfect channel state information on CDS by considering the CSI feedback delay.

We show that localized subcarrier allocation yields highest aggregate data throughput for CDS. We also show that localized mapping is very sensitive to the quality of CSI and the capacity gain quickly decreases for very fast changing channel. For high mobility users, distributed subcarrier mapping with static round-robin scheduling is more suitable.

The analysis explores the effect of adaptive modulation but does not consider channel coding. Future work will examine the effects of hybrid automatic repeat request (ARQ) schemes [22].

REFERENCES

[1] S. Grandhi, R. Yates, and D. J. Goodman, "Resource Allocation for Cellular Radio Systems," *IEEE Trans. Veh. Technol.*, vol. 46, no. 3, Aug. 1997, pp. 581-587.

[2] L. Jorguseki, J. Farserotu, and R. Prasad, "Radio Resource Allocation in Third-Generation Mobile Communication Systems," *IEEE Commun. Mag.*, vol. 39, no. 2, Feb. 2001, pp. 117-123.

[3] S. Nanda, K. Balachandran, and S. Kumar, "Adaptation Techniques in Wireless Packet Data Services," *IEEE Commun. Mag.*, vol. 38, no. 1, Jan. 2000, pp. 54-64.

[4] J. K. Cavers, "Variable-Rate Transmission for Rayleigh Fading Channels," *IEEE Trans. Commun.*, vol. COM-20, no. 1, Feb. 1972, pp. 15-22.

[5] A. Goldsmith and S. G. Chua, "Adaptive Coded Modulation for Fading Channels," *IEEE Trans. Commun.*, vol. 46, no. 5, May 1998, pp. 595-602.

[6] H. G. Myung, J. Lim, and D. J. Goodman, "Single Carrier FDMA for Uplink Wireless Transmission", *IEEE Vehicular Technology Mag*., vol. 1, no. 3, Sep. 2006, pp. 30-38.

[7] H. G. Myung, J. Lim, and D. J. Goodman, "Peak-to-average Power Ratio of Single Carrier FDMA Signals with Pulse Shaping", *Proc. IEEE International Symposium on Personal, Indoor and Mobile Radio Communications (PIMRC)* 2006, Sep. 2006.

[8] H. Ekström, A. Furuskär, J. Karlsson, M. Meyer, S. Parkvall, J. Torsner, and M. Wahlqvist, "Technical Solutions for the 3G Long-Term Evolution," *IEEE Commun. Mag*., vol. 44, no. 3, Mar. 2006, pp. 38-45.

[9] D. Falconer, S. L. Ariyavisitakul, A. Benyamin-Seeyar, and B. Eidson, "Frequency Domain Equalization for Single-Carrier Broadband Wireless Systems," *IEEE Commun. Mag.*, vol. 40, no. 4, Apr. 2002, pp. 58-66.

[10] M. Tüchler and J. Hagenauer, "Linear Time and Frequency Domain Turbo Equalization," *Proc. IEEE 53rd Veh. Technol. Conf. (VTC)*, vol. 2, May 2001, pp. 1449-1453.

[11] F. Pancaldi and G. M. Vitetta, "Block Channel Equalization in the Frequency Domain," *IEEE Trans. Commun.*, vol. 53, no. 3, Mar. 2005, pp. 463-471.

[12] N. Benvenuto and S. Tomasin, "Iterative Design and Detection of a DFE in the Frequency Domain," *IEEE Trans. Commun.*, vol. 53, no. 11, Nov. 2005, pp. 1867-1875.

[13] U. Sorger, I. De Broeck, and M. Schnell, "Interleaved FDMA - A New Spread-Spectrum Multiple-Access Scheme," *Proc. IEEE ICC '98*, Atlanta, GA, Jun. 1998, pp. 1013-1017.

[14] J. Lim, H. G. Myung, K. Oh, and D. J. Goodman, "Channel-Dependent Scheduling of Uplink Single Carrier FDMA Systems," *IEEE Vehicular Technology Conference (VTC) 2006 Fall*, Montreal, Canada, Sep. 2006.

[15] J. Lim, H. G. Myung, K. Oh, and D. J. Goodman, "Proportional Fair Scheduling of Uplink Single-Carrier FDMA Systems," *The 17th Annual IEEE International Symposium on Personal, Indoor and Mobile Radio Communications (PIMRC '06)*, Helsinki, Finland, Sep. 2006.

[16] D. J. Goodman and N. B. Mandayam, "Power Control for Wireless Data," *IEEE Personal Commun.*, vol. 7, no. 2, Apr. 2000, pp. 48-54.

[17] B. Sklar, "Rayleigh Fading Channels in Mobile Digital Communication Systems: Part I: Characterization," *IEEE Commun. Mag.*, vol. 35, no. 7, Jul. 1997, pp. 90-100.

[18] Motorola, "Simulation Methodology for EUTRA UL: IFDMA and DFT-Spread-OFDMA," *3GPP TSG-RAN WG1 #43*, Technical Document R1-051335, Nov. 2005.

[19] 3GPP TS 45.005 – 3GPP; Technical Specification Group GSM/EDGE Radio Access Network; Radio Transmission and Reception (Release 7).

[20] D. J. Goodman, Z. Marantz, P. Orenstein, and V. Rodriguez, "Maximizing the Throughput of CDMA Data Communications", *IEEE Vehicular Technology Conference (VTC) 2003 Fall*, Orlando, Florida, Oct. 2003.

[21] A. J. Goldsmith and S.-G. Chua, "Variable-Rate Variable-Power MQAM for Fading Channels," *IEEE Trans. Commun.*, vol. 45, no. 10, Oct. 1997, pp. 1218-1230.

[22] M. A. Kousa and M. Rahman, "An Adaptive Error Control System Using Hybrid ARQ Schemes," *IEEE Trans. Commun.*, vol. 39, no. 7, Jul. 1991, pp. 1049-1057.

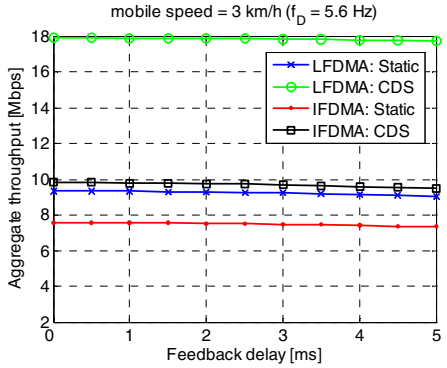

(a)

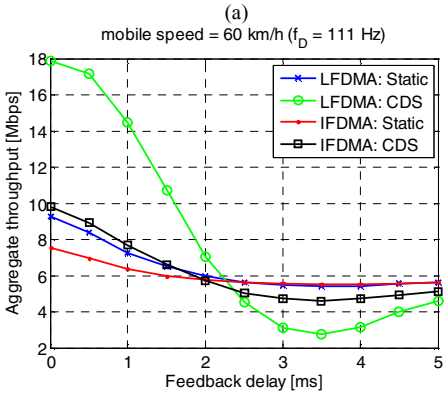

(b)

Figure 5: Aggregate throughput with CDS and adaptive modulation; (a) mobile speed = 3 km/h (Doppler = 5.6 Hz); (b) mobile speed = 60 km/h (Doppler = 111 Hz).

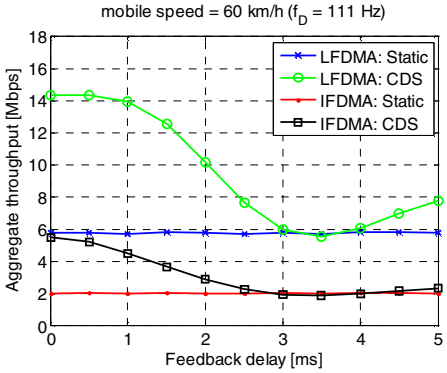

Figure 6: Aggregate throughput with CDS and constant modulation (16-QAM) with mobile speed of 60 km/h.

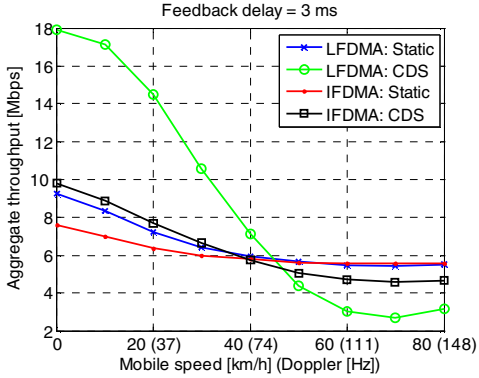

Figure 7: Aggregate throughput with CDS and adaptive modulation with feedback delay of 3 ms and different mobile speeds.